KnE Engineering

STARTCON19
STARTCON19 - International Doctorate Students Conference + Lab Workshop in Civil Engineering
Volume 2020

Conference Paper

The Effect of the Activator/Precursor Ratio on the Rheological Properties of the Alkali-activated Mining Waste Mud Paste

Abdelhakim Benhamouda, João Castro-Gomes, and Luiz Pereira-de-Oliveira

Centre of Materials and Building Technologies (C-MADE/UBI), Department of Civil Engineering and Architecture, University of Beira Interior (UBI), 6201-001 Covilhã, Portugal

Abstract

To determine the properties of paste, mortar or concrete, it is necessary to understand its rheological behaviour first. This study discusses the effect of the activator/precursor ratio on the rheological properties of the alkali-activated paste. The pastes consisted of a mix of 70 % of tungsten mining waste mud, 15% waste glass and 15% of metakaolin. This mix was activated by combining sodium hydroxide and sodium silicate. Five activator/precursor (a/p) ratios were studied: 0.37, 0.38, 0.39, 0.40 and 0.41. The result obtained shows that the rheology of the pastes is affected by the activator/precursor ratio. The rheological behaviour of the paste fits the Bingham model. The yield stress (τ_0) and plastic viscosity (μ) increase inversely with the activator/precursor ratio (e.g. a/p=0.37 gives τ_0=84.19 and μ=0.4185; a/p=0.41 gives τ_0=30.389 and μ=0.2937). The workability increases proportionally with the activator/precursor ratio (e.g. a/p=0.37 gives a slump=133 mm; a/p=0.41 gives a slump=158 mm). The compressive strength decreases when the activator/precursor ratio increases (e.g. at 28 days for a/p=0.37, the compressive strength was 19.6 MPa; for a/p=0.41, the compressive strength was 13 MPa). Finally, the ideal ratios were 0.38 and 0.39.

Corresponding Author:
Abdelhakim Benhamouda
benhamouda.abdelhakim@gmail.com

Received: 7 January 2020
Accepted: 21 April 2020
Published: 3 May 2020

Publishing services provided by Knowledge E

Selection and Peer-review under the responsibility of the STARTCON19 Conference Committee.

1. Introduction

Currently, the building industry is facing a great challenge: the protection of the environment and the usage of waste and recycled materials [1]. The production of Portland cement (PC) is responsible for the emission of between 6% to 8% of CO_2 greenhouse gases [2]. Besides, in Europe, there is a major concern about the quantity and diversity of hazardous solid waste production.

The increasing concern about the environmental consequences of waste disposal has led to new investigations on new utilization (reuse) possibilities. For example, large quantities of sludge and by-products, such as fly ash, are produced during the combustion of coal used for electricity generation [3]. Also, in Europe, mining and quarrying industry waste are very relevant. These activities produce about 55% of the total industrial wastes according to recent Eurostat data [4].

For a better understanding of the behaviour and performance of the alkali-activated (AA) materials, it is important to study their rheological properties for the manufacturing of AA-based products.

Rheology is the study of the fluidity and deformation of matter in the fresh or hardened state, and the emphasis on flow means that it is concerned with the relationship between stress, strain, rate of strain, and time [5].

In (PC), the rheological testing, using a viscometer to break down the interparticle forces formed by the hydration of cement grains, consists in exposing the pastes to shear stress with known shear rates.

Several different models describe the rheological behaviour of cement pastes. Generally, the cement paste fits the Bingham model[5] Eq. (1), as presented as follows. The Bingham model:

$$\tau = \tau_0 + \mu\gamma \tag{1}$$

Where

τ: shear stress,

τ_0: yield stress,

μ: plastic viscosity and

γ: shear rate.

Other models can be used to analyse the rheological behaviour of cement pastes, such as the Ostwald de Waele and the Herschel–Bulkley models equations. (2) and (3), respectively, as presented next (Tattersall GH, 1983).

The Ostwald de Waele model:

$$\tau = k\gamma^n \tag{2}$$

The Herschel-Bulkley model:

$$\tau = \tau_0 + k\gamma^n \tag{3}$$

Where

k: the consistency coefficient (Pa.s^n), and

n: the dimension less fluidity index.

Besides the studies on the rheology of cement pastes, there are a few studies on the rheology of alkali-activated materials. Such main research studies are presented in Table.1. Since the purpose of this paper is to contribute to the knowledge of this scientific field, a short review of the existing studies on the rheology of AA materials is presented next.

TABLE 1: Some research activities regarding the rheology of alkali-activated materials (2010 to 2016).

Studies	References
Rheological behavior of fly ash-based geopolymer concrete	[7]
Rheological behavior of alkali-activated Metakaolin during geopolymerization	[8]
Rheology of geopolymer by DOE approach	[9]
Rheological properties of alkaline-activated fly ash used in jet grouting applications	[10]
The interrelationship between surface chemistry and rheology in alkali activated slag paste	[11]
Rheological behavior of a fresh geopolymer based on Metakaolin: Effect of the introduction of calcium carbonate	[12]
Rheology of alkali-activated slag pastes. Effect of the nature and concentration of the activating solution	[13]
Observations on the rheological response of alkali activated fly ash suspensions: the role of activator type and concentration	[14]
Alkali-activated slag cements using waste glass as alternative activators. Rheological behavior	[6]

Puertas et al [12] compared the rheological parameters of PC and AA materials, namely the concentration of alkali solutions. Torres-Carrasco et al. concluded that the rheological behaviour of alkali-activated slags pastes fitted the Herschel-Bulkley model when the activator was a commercial water glass solution or NaOH/Na_2CO_3 combined with waste glass [14].

This study aims to discuss the role of the a/p on the rheological parameters in fresh and hardened state and choose the ideal ratio, which is the one that has the best behaviour in a fresh state with good mechanical performance.

2. Materials and Methods

2.1. Materials

The materials used in this study to prepare the AA paste were Metakaolin (Mk), tungsten mining waste mud (TMWM) and waste glass (WG) as a precursor. The metakaolin was supplied by BASF with the reference name “MASTERLIFE Mk”, mud waste was collected from the Panasqueira tungsten mine located in Covilhã, Portugal, and the waste glass was obtained by crushing glass bottles. The chemical composition (determined by SEM-EDX) is given in Table 2 and the physical properties (bulk density and Blaine finesses) are presented in Table 3.

The sodium hydroxide (SH), NaOH, and sodium silicate (SS), Na_2SiO_3, are the activators. The sodium hydroxide solution was prepared by dissolving sodium hydroxide

Table 2: Chemical composition of (Mk), (TMWM) and (WG) in %.

Chemical composition	Mud waste	Glass	Metakaolin
Na_2O	0.85	12.52	0.32
SiO_2	46.67	68.13	52.28
Al_2O_3	17.01	2.80	42.99
K_2O	4.90	0.86	0.94
CaO	0.69	10.52	/
SO_3	7.90	0.23	/
Fe_2O_3	15.47	2.90	1.49
MgO	4.83	2.04	0.47

Table 3: Physical properties of (Mk), (TMWM) and (WG).

Physical properties	Mud waste	Glass	Metakaolin
Bulk density(g/cm^3)	3.10	2.49	0.2683
Blaine fineness (cm^2/g)	742	2665	4467

pellets (98% purity obtained from Fisher Scientific, Schwerte, Germany) in deionized water and allowed to cool before use. Sodium silicate was obtained from Solvay SA, Póvoa de Santa Iria, Portugal. Table 4 presents the chemical composition and density of activators by weight.

Table 4: Chemical composition and density of (SH) and (SS) in %.

Chemical composition	Sodium hydroxide	Sodium silicate
Na_2O	13.02	19.37
SiO_2	0.00	62.60
Al_2O_3	0.00	0.90
H_2O	43.27	142.32
Density (g/cm^3)	1.0192	1.5725

2.2. Methods

2.2.1. Synthesis of samples

The AA paste was a mix of 70% (TMWM), 15% (WG) and 15% (Mk) mixed in the dry state for 5 min to assure the homogeneity of our precursor. The (NaOH) with a molarity =10M and (Na_2SiO_3) were mixed for 3 to 5 minutes to form our activator.

The alkali-activator solution with a ratio (Na_2SiO_3)/ (NaOH) =4 was added to the precursor. The paste was stirred for 2.5 min at 200 rpm, followed by 2.5 min at 400

rpm at a temperature of 20°C for different activator/precursor (a/p) ratios, namely 0.37, 0.38, 0.39, 0.40 and 0.41.

2.2.2. Determination of rheological parameters

For the rheological study, a Viskomat NT rheometer (Rheometer for mortar and paste, produced by Schleibinger Testing Systems) was used. This apparatus automatically measures a series of data points of torque (T) and speed (N).

Immediately after mixing the paste, it was transferred into the rheometer cup to start measuring the rheological parameters.

In the Viskomat NT rheometer, as the cylindrical sample container rotates (Fig.1), the paste flows through the blades of the impeller and exerts a torque which is measured by a transducer. For the testing conditions, the rotation speed of the container was set to vary with time as a ramp speed profile. In the ramp profile (Fig. 2), the rotation speed was adjusted to vary with time, increasing from an initial value of zero to 120 rpm for 5 minutes and then decreasing from 120 rpm to zero in other 5 minutes. This speed profile was used to determine plastic viscosity and yield stress-related coefficients (μ and τ_0, respectively).

2.2.3. Paste fluidity (mini slump)

The paste fluidity was determined with the mini-slump test [15] on the samples, 7, 16, 25, 34 and 52 min after mixing. The slump cone has an upper diameter of 19 mm, a lower diameter of 38.1 mm, and a height of 57.2 mm. The cone is positioned in the center of the plate. After pouring the paste into the cone without causing it to overflow, the upper part of the cone is tamped lightly to bleed off any entrapped air pockets, and the cone is then gently lifted. After the pastes were dropped 10 times on a flow table, the diameter was measured in three directions: the values used were the arithmetic means of these measurements. Fig. 3 presents a spread of the paste with a/p= 0.41.

2.2.4. Compressive strength

The compressive strength tests were performed on a 3000 KN electro-hydraulic mechanical testing machine, the “ADR Touch 3000 BS EN Compression Machine with Digital Readout and Self Centring Platens”, in accordance with EN 196-1. Compressive strength data was obtained from testing five specimens with 25 mm cubic in size.

Figure 1: View of AA paste during rheology test on the rheometer.

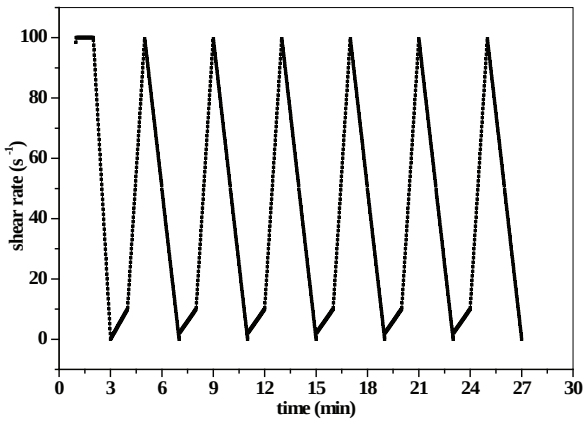

Figure 2: Ramp speed time profile for Viskomat NT rheometer.

3. Results and Discussion

The influence of the a/p ratio on the rheological behaviour of the AA paste is discussed in two parts in this section: fresh and hardened states.

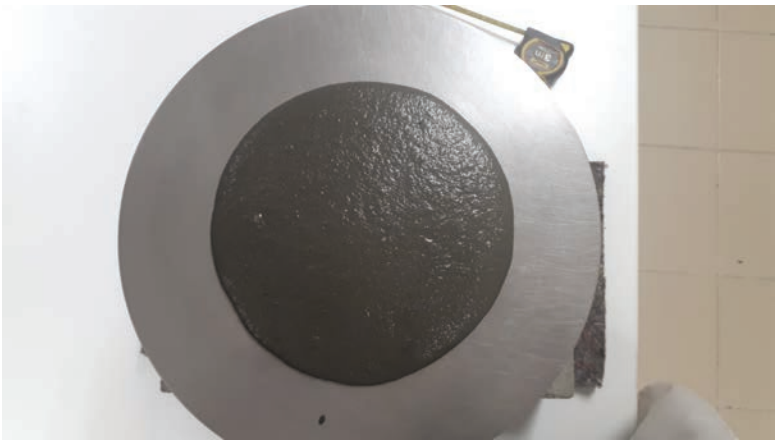

Figure 3: Spread of the paste with a/p =0.41.

3.1. Fresh state

3.1.1. Evaluation of torque and rotational speed

Fig. 4 presents the changes of torque versus rotational speed of the AA pastes for different a/p ratios. From the graph, it can be observed that all the pastes tested fit the Bingham model (Eq (1)). Also, it can be seen that the increase of torque along with the increase of rotational speed, for example in the mix 0.41, needs a smaller torque (around 97.433327 N.mm). In opposition, mix (a/p) =0.37 needs the highest torque (170.53838 N.mm). These results are explained by the following: when the paste is very liquid, the stress to break the interparticle forces is smaller when compared to a higher viscous paste.

The results obtained in our study are comparable to the results obtained by other authors using slag-based AA pastes [12]. However, their study was based on changing the activator concentration while in this study this parameter was kept constant and the a/p ratios varied from 0.37 to 0.41.

3.1.2. Evaluation of yield stress

The relative yield stress was graphically determined from the curve of torque versus rotational speed. Fig. 5 shows such results. It is verified that the relative yield stresses of the mixes increases with time which is explained by the formation of C-S-H gel (the paste is more hardened; for example, in the first 7 min, the value of yield stress in the paste with the 0.37 a/p ratio was 84.19 N.mm and became 98.368 N.mm in 52 min). In opposition, it was observed that the increase of the a/p ratios lets the relative yield stress decrease which is explained with the decrease of the interparticle forces between

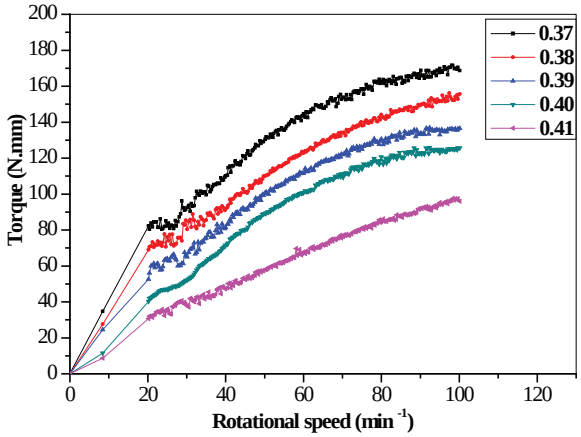

Figure 4: Torque versus rotational speed.

grains of paste (for the ratio a/p= 0.37, the yield stress was 98.368 N.mm in 52 min, but in the 0.41 a/p was 40.084 N.mm in the same time).

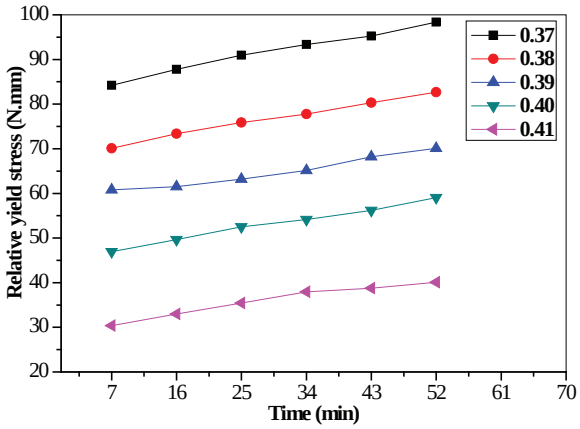

Figure 5: Relative yield stress versus time.

3.1.3. Evaluation of relative plastic viscosity

In the presented models, many factors affect the viscosity. The solid content and the interparticle forces between particles are one of these factors. The relative viscosity can be described by the empirical expression, proposed by [16], as follows:

Eq:

$$\mu = \mu_0 \quad (1 - (\Phi/\Phi_{max}))^n \tag{4}$$

Where μ_0 is the solution viscosity, Φ is the actual solid volume fraction Φ_{max} is the maximum solid volume fraction.

The variation of plastic viscosity versus the time in different a/p ratios is represented in Fig. 6. The graph shows that the relative plastic viscosity increases with the decrease

of the a/p ratio and increases proportionally with time. This can be explained due to the solid content and the stress to break the interparticle forces: the plastic viscosity increases for pastes with a lower liquid phase which requires higher stress to break the interparticle forces and higher value of solid content (Eq (4)). For example, the paste with a 0.38 a/p ratio after 52 min has a higher value of plastic viscosity (0.4696 N.mm.min) than the paste with a 0.40 a/p ratio (0.3989 N.mm.min).

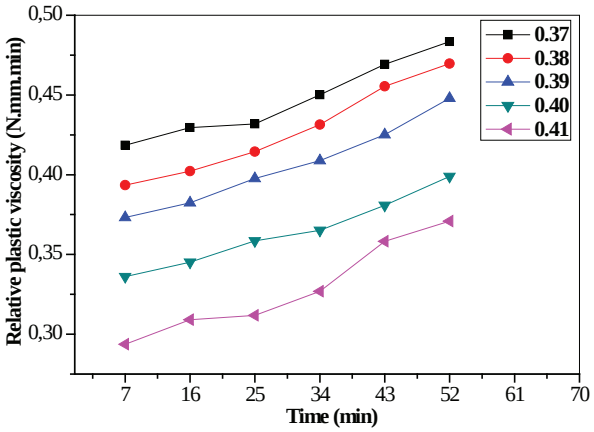

Figure 6: Relative plastic viscosity versus time.

3.1.4. Slump flow

Fig. 7 shows the variation of the slump (fluidity) of different pastes with a different ratio of a/p versus time. From this graph, the reduction of the slump diameter with time and the decrease of a/p ratios can be observed. This reduction of the diameter of the slump occurs due to the formation of C-S-H gel with time (the paste is more hardened, 145 mm for the paste with a 0.39 a/p ratio in 7 that becomes 126 after 52 min).

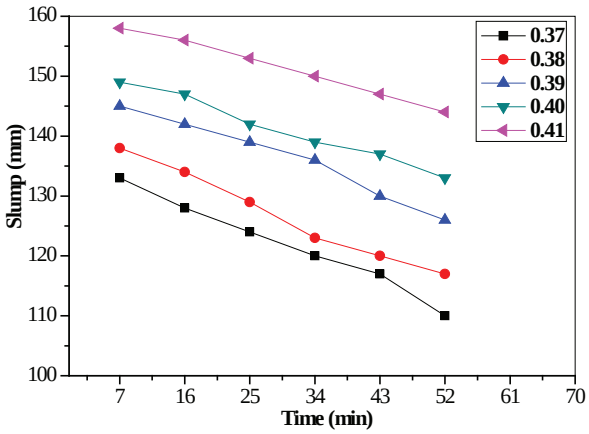

Figure 7: Slump versus time.

3.2. Hardened state

3.2.1. Compressive strength

Fig. 8 presents the compressive strength results measured at 7, 14, and 28 days. When comparing the results obtained for the different mixtures, it was observed that the compressive strength decreased with the increase of a/p ratios. This can be explained by the increase of paste porosity which represents a compressive strength reduction of about 35% at 28 days for 0.37 to 0.41 a/p ratios, Moreover, it also decreases because of the increase of the a/p influence on the cohesion between the grains of the paste.

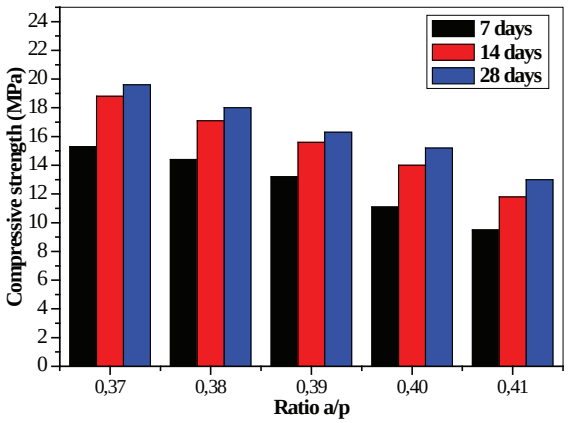

Figure 8: Compressive strength as a function of the a/p ratio.

4. Conclusions

This paper experimentally investigated the rheological properties of AA pastes of different mixes of tungsten mining waste mud, grounded waste glass and metakaolin. All mixes were activated using sodium hydroxide and sodium silicate. The main conclusions that can be drawn from this study are listed below:

1. The rheological behaviour in AAM pastes fits the Bingham model. The torque increases proportionally with the increase of rotational speed. Besides, the torque x rotational speed curves were found to be dependent on the activator/precursor ratios (i.e. the increase in the activator/precursor offset increased torque and relative yield stress).
2. The relative yield stress and relative plastic viscosity increased inversely with the increase of the a/p ratio and proportionally with time. This can be explained by the solid content of the mixes and the quantity of the liquid activator used (i.e. more

liquid decreases the interparticle forces that are needed to break the interstitial cohesion).

3. The workability (fluidity) decreases with the decrease of the a/p. This can be explained by the decrease of the cohesion between the grains of the paste.
4. The compressive strength was affected inversely by the a/p ratio (the increase of compressive strength with the decrease in the a/p ratio). This can be explained by the increase in paste porosity.
5. Finally, the ideal a/p ratios in this study were a/p=0.38 and a/p=0.39 because these ratios have a higher mechanical performance with good rheological behaviour in the fresh state.

Acknowledgement

This work was partially financed by Portuguese national funds through FCT – Foundation for Science and Technology, IP, within the research unit C-MADE, Centre of Materials and Building Technologies (CIVE-Central Covilhã-4082), University of Beira Interior, Portugal.

References

[1] European Parliament, Council Directive 2013/59/Euratom of 5 December 2013 laying down basic safety standards for protection against the dangers arising from exposure to ionising radiation, and repealing Directives 89/618/Euratom, 90/641/Euratom, 96/29/Euratom, 97/43/Euratom a. *Off J Eur Commun L13*, (2014) 1–73. https://doi.org/doi:10.3000/19770677.L_2013.124.eng.

[2] M. C. Bignozzi, S. Manzi, M. E. Natali, W. D. A. Rickard, & A. Van Riessen, Room temperature alkali activation of fly ash: The effect of Na 2O/SiO2 ratio. *Construction and Building Materials*, **69** (2014) 262–270. https://doi.org/10.1016/j.conbuildmat.2014.07.062.

[3] R. B. V. Hardjito D., Wallah S. E. Sumajouw D.M.J., On the Development of Fly AshBased Geopolymer Concrete. *ACI Materials Journal/November-December*, (2004) 467–472.

[4] J. P. Castro-Gomes, A. P. Silva, R. P. Cano, J. Durán Suarez, & A. Albuquerque, Potential for reuse of tungsten mining waste-rock in technical-artistic value added products. *Journal of Cleaner Production*, **25** (2012) 34–41. https://doi.org/10.1016/j.jclepro.2011.11.064.

[5] G. H. Tattersall & P. F. G. Banfill, *The rheology of fresh concrete* (Pitman Advanced Publishing Program, 1983).

[6] R. Bhattacharjee & A. I. Laskar, Rheological behavior of fly ash based geopolymer concrete. *35th Conference on OUR WORLD IN CONCRETE & STRUCTURES*, (2010).

[7] A. Poulesquen, F. Frizon, & D. Lambertin, Rheological behavior of alkali-activated metakaolin during geopolymerization. *Cement-Based Materials for Nuclear Waste Storage*, **357** (2011) 225–238. https://doi.org/10.1007/978-1-4614-3445-0_20.

[8] M. Romagnoli, C. Leonelli, E. Kamse, & M. Lassinantti Gualtieri, Rheology of geopolymer by DOE approach. *Construction and Building Materials*, **36** (2012) 251–258. https://doi.org/10.1016/j.conbuildmat.2012.04.122.

[9] N. Cristelo, E. Soares, I. Rosa, T. Miranda, D. V. Oliveira, R. A. Silva, & A. Chaves, Rheological properties of alkaline activated fly ash used in jet grouting applications. *Construction and Building Materials*, **48** (2013) 925–933. https://doi.org/10.1016/j.conbuildmat.2013.07.063.

[10] A. Kashani, J. L. Provis, G. G. Qiao, & J. S. J. Van Deventer, The interrelationship between surface chemistry and rheology in alkali activated slag paste. *Construction and Building Materials*, **65** (2014) 583–591. https://doi.org/10.1016/j.conbuildmat.2014.04.127.

[11] A. Aboulayt, M. Riahi, S. Anis, M. O. Touhami, & R. Moussa, Rheological behavior of a fresh geopolymer based on metakaolin: effect of the introduction of calcium carbonate. *International Journal of Innovation and Applied Studies*, **7** (2014) 1170–1177.

[12] F. Puertas, C. Varga, & M. M. Alonso, Rheology of alkali-activated slag pastes. Effect of the nature and concentration of the activating solution. *Cement and Concrete Composites*, **53** (2014) 279–288. https://doi.org/10.1016/j.cemconcomp.2014.07.012.

[13] K. Vance, A. Dakhane, G. Sant, & N. Neithalath, Observations on the rheological response of alkali activated fly ash suspensions: the role of activator type and concentration. *Rheologica Acta*, **53** (2014) 843–855. https://doi.org/10.1007/s00397-014-0793-z.

[14] M. Torres-Carrasco, C. Rodríguez-Puertas, M. Del Mar Alonso, & F. Puertas, Alkali activated slag cements using waste glass as alternative activators. Rheological behaviour. *Boletin de la Sociedad Espanola de Ceramica y Vidrio*, **54** (2015) 45–57. https://doi.org/10.1016/j.bsecv.2015.03.004.

[15] P. A. Wedding & D. L. Kantro, Influence of Water-Reducing Admixtures on Properties of Cement Paste-A Miniature Slump Test. *Cement Concrete and Aggregates*, **2** (1980). https://doi.org/10.1520/CCA10190J.

[16] I. M. Krieger & T. J. Dougherty, A Mechanism for Non-Newtonian Flow in Suspensions of Rigid Spheres. *Transactions of the Society of Rheology*, **3** (1959) 137–152. https://doi.org/10.1122/1.548848.